A Low-Profile Electrically Small Serrated Rectangular Patch Antenna for RFID Applications

Naveen Kumar Majji
Department of ECE, KLEF, India | Department of ECE, PSCMR College of Engineering and Technology, India
navvenkumarmajji@gmail.com

Venkata Narayana Madhavareddy
Department of ECE, KLEF, India
mvn@kluniversity.in

Govardhani Immadi
Department of ECE, KLEF, India
govardhanee_ec@kluniversity.in (corresponding author)

Navya Ambati
Department of ECE, KLEF, India
ambatinavya88@gmail.com

ABSTRACT

This paper presents the design and analysis of a global system for mobile communication applications, as well as the design and analysis of a compact, bidirectional Electrically Small Antenna (ESA) at 0.9 GHz for Radio Frequency Identification (RFID) applications. In order to attain results at lower frequencies while keeping a compact size, the proposed design consists of a microstrip patch antenna in which an SRR and a semicircular-shaped SRR were subtracted from the ground plane. The dimensions of the FR4 substrate, on which this ESA was designed, were $20 \times 18 \times 1.6$ mm. Ansys HFSS was used for the design and simulation of the antenna. Chemical etching was implemented to fabricate the ESA and MS2037C Anritsu Combinational Analyzer was applied for testing. The simulated results show that at 0.9 GHz, the ESA achieves a bandwidth of 300 MHz (700 MHz-1000 MHz). At the resonance frequency, a bidirectional radiation pattern with a 80% radiation efficiency is obtained in both H and E planes. A 90% agreement between the simulated and the fabricated results has been achieved.

Keywords-electrically small antenna; gain; Chu limit; reflection coefficient; VSWR

I. INTRODUCTION

Electrically Small Antennas (ESAs) play an important role in modern communication engineering as the requirement for miniaturization is growing day by day. An antenna which is enclosed completely in a sphere with radius a is treated as an ESA. For such an antenna Ka<1, where Ka is a wave number equal to $2\pi/\lambda$, where λ is the free space wavelength. Normally, if an antenna has dimensions (including any ground plane) less than $\lambda/4$, it is often referred to as an ESA. ESAs tend to be less efficient and more challenging to design than antennas of normal size. Also, reducing the antenna size, results in larger input reactance, smaller radiation resistance, poor radiation efficiency, and narrow impedance bandwidth. Being smaller in size, ESAs are easily integrated into smaller devices and have a simple structure, but they suffer from low radiation resistance and high reactance due to their shorter electrical length. Because of the larger wavelength of the EM waves in this frequency band, it is demanded to reduce the antenna size, which in turn requires the use of ESAs. A meander line is placed in order to decrease the size and achieve good impedance matching at 2.4 GHz. The former is designed by employing a characteristic mode theory, according to which this line should have dimensions 8 mm × 8 mm × 1.5 mm [2]. A low-cost, uniplanar, electrically small structure antenna is proposed in [3] with size $0.154 \times 0.154 \times 0.0004 \lambda^3$ and Ka =0.68,

to achieve minimum return loss and efficient radiation patterns [3]. An electrically small, low-profile antenna supporting both linear and circularly polarized waves plus rectification at 915 MHz in the ISM band with less quality factor for wireless power transfer technologies in the IOT applications is designed in [4]. Authors in [5, 7] proposed a novel ESA using DAM techniques to improve the bandwidth and Q factor of the antenna. Authors in [8] presented a small monopole antenna design for super-wideband (SWB) applications. An antenna was constructed based on a trapezoid form radiator, triangle tapered feed line, and semi-circular ground, to produce good broad frequency bandwidth at the resonating frequency of 1.42 GHz. The reactive impedance problem can be overcome by constructing an antenna with an embedded non-foster circuit for Negative Impedance Conversion (NIC) [9]. In order to optimize and reduce the size of the antenna, active circuits were placed inside the antenna. An ESA for GNSS terminals was proposed in [10], in which a dielectric block with more permittivity was used to achieve miniaturization. In [11], a multi-band, wireless USB dongle ESA with low profile was suggested to operate at LTE 700 and 1.6 GHz. An ESA with a compact size of 4 mm ×4 mm and with a circular shape slot which resulted in an improvement of broad band characteristics was proposed in [13]. An Ultra-High Frequency (UHF) radio frequency identificator that comprised a C-shaped structure with a diameter of 41 mm and thickness of 6.48 mm was introduced in [14]. The proposed Tunable Bio Metric Antenna Array (BMAA) in [15], consisted of two quarter wave closely-spaced monopoles operating at 600 MHz.

From the aforementioned studies, it can be concluded that the suggested ESAs either had complicated structures covering large regions, or they did not cover the 900 MHz frequency range for GSM and RFID applications. The proposed design consists of a microstrip patch antenna in which an SRR and a semicircular shaped SRR were subtracted from the ground plane to obtain results at lower frequencies by maintaining a compact size. Wide impedance bandwidth of 0.3 GHz (0.7 GHz – 1.0 GHz) was obtained for a single band ESA. The return loss of the single band is -23 dB at 0.9 GHz with VSWR < 2. The recommended antenna has 61.7% radiation efficiency and the significant peak gain of 1 dB. Additionally, in both E and H planes, the serrated rectangular ESA offers a bidirectional radiation pattern.

II. ESA DESIGN METHODOLOGY AND GEOMETRY

The serrated rectangular ESA is created by starting with a rectangular patch antenna and applying fundamental microstrip patch antenna design principles, and finally modifying its shape to meet the required parameters. The rectangular patch antenna has good return loss only in a particular frequency range. This simple patch antenna design has undergone a few modifications to get the resonant band at 900 MHz. As a substrate, FR4 epoxy material measuring 1.6 mm in height was used. The proposed antenna has a size of 20×18 mm² and it is fed with a 50 Ω microstrip transmission line. In iteration 1, the basic shape of a rectangular shaped SRR is designed with 12 mm length (L1) and width (W1) using the HFSS. Another rectangular shaped patch antenna with L2 = 16 mm and W2 = 15 mm is added in iteration II. In iteration III, along with the

rectangular SRR, a rectangular micro strip and a semi-circular shaped SRR are placed at the bottom of the design. The semi-circular SRR has a radius of 7 mm. In iteration IV, along with the rectangular shaped slot, a stub is added on the left side and in iteration V, rectangular 0.5 mm slots are placed to improve the antenna performance. As per the fundamental limit of ESA, the Ka value for the designed ESA is 0.87. Figures 1-5 represent the iterations I-V of the antennas along with their return loss in dB. The mathematical formulas that are utilized in manufacturing the proposed ESA are shown below. The dimensions of the microstrip patch antenna were calculated by utilizing the concept behind the theory of the transmission lines. The width of the patch can be estimated by:

$$W = \frac{V_o}{2F_r}\sqrt{\frac{2}{\varepsilon_r+1}} \qquad (1)$$

The length of the patch can be calculated by (2), where ε_{reff} is the effective dielectric constant of the substrate.

$$L = \frac{C}{2F_r\sqrt{\varepsilon_{reff}}} - 2\Delta l \qquad (2)$$

$$\Delta l = 0.412h\frac{(\varepsilon_{reff}+0.03)(w+0.26h)}{(\varepsilon_{reff}-0.258)(w+0.8h)}$$

The dielectric constant of the substrate is:

$$\varepsilon_{reff} = \frac{\varepsilon_r+1}{2} + \frac{\varepsilon_r-1}{2}\left[1 + \left[\frac{12h}{w}\right]\right]^{-1/2} \qquad (3)$$

These models are very small in size and easy to fabricate. The step-by-step design procedure of creating an ESA is shown in Figure 1. The dimensions used in designing the ESA are shown in Table I.
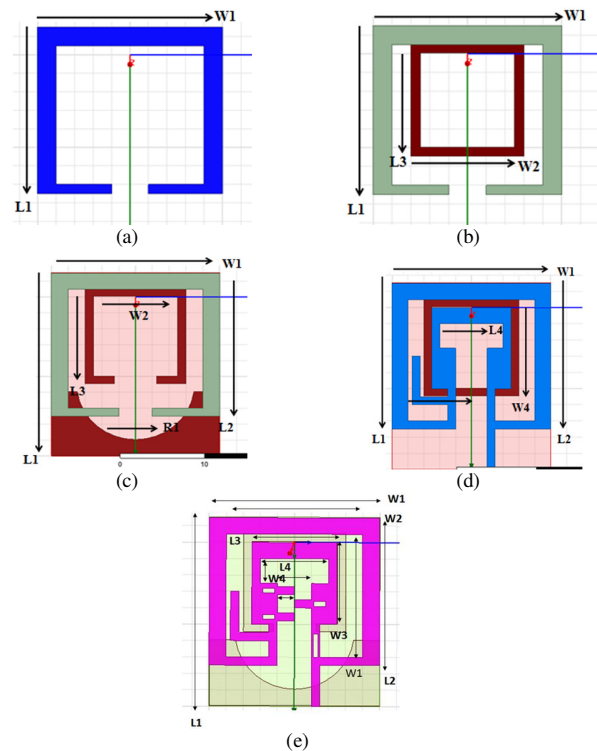

Fig. 1.   Iterations of the serrated rectangular ESA.

TABLE I.   DIMENSIONS OF DGS SRR

Parameter	Value (mm)	Parameter	Value (mm)
L1	20	L_3	10
W1	18	W_3	10
L2	16	L_4	8
W2	15	W_4	4
S1, S2	0.5	S3, S4	0.5
		R1	7

The prototype of the serrated rectangular ESA is displayed in Figure 2(a)-(b) and Figure 2(c) depicts the measurement setup for the antenna with MS2037C Anritsu combinational Analyzer. Figure 3 exhibits the setup for gain and radiation pattern in an anechoic chamber.

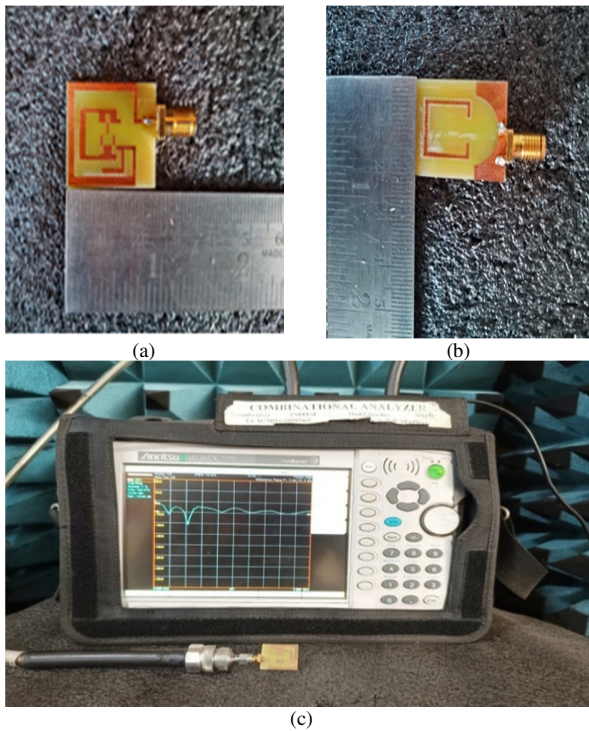(a)   (b)

(c)

Fig. 2.   Serrated Rectangular ESA prototype. (a) Top view, (b) bottom view, (c) measurement setup with the MS2037C Anritsu Combinational Analyser.
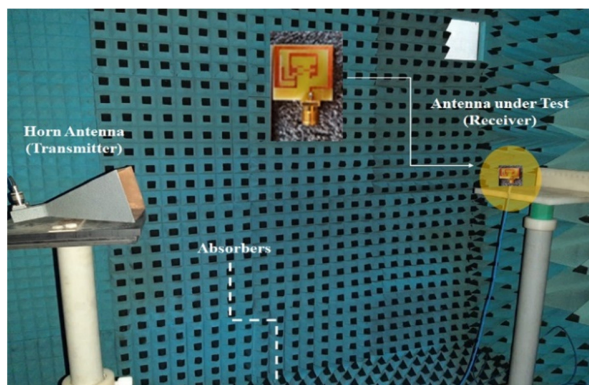

Fig. 3.   Gain and radiation pattern measurement in anechoic chamber.

Figure 4 portrays the S11 of the serrated rectangular microstrip antenna. In iteration 1, the ESA operates at 1.13 GHz with a return loss of -21 dB. In iteration 2, the ESA operates at 1 GHz with S11 of -21 dB, in iteration 3 it operates at 1.0 GHz with S11 of -20 dB, in iteration 4, it operates at 0.94 GHz with S11 of -21 dB, and in iteration 5 the serrated rectangular ESA with DGS operates at 0.9 GHz with S11 = -23 dB which is suitable for GSM and RFID applications.
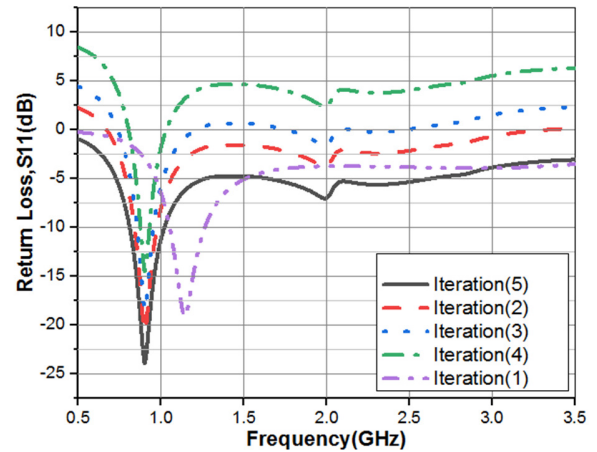

Fig. 4.   Return loss of the serrated rectangular ESA for all the iterations.

III.   RESULTS AND DISCUSSION

The HFSS-IE employs the Method of Moments (MoM), while Ansys Electronic Desktop's simulation of the serrated rectangular ESA is based on the finite element approach. The boundary box had dimensions 100 mm × 100 mm × 50 mm and the antenna was simulated through a lumped port. A prototype of the serrated rectangular ESA was fabricated (Figure 2) to validate the accuracy of the simulation results. The combinational analyzer MS2037C was used to measure the reflection coefficient S11. The variation of S11 with respect to frequency of the serrated rectangular ESA is displayed in Figure 5. The fabricated antenna's results demonstrate that the antenna exhibits a resonance frequency at 0.9 GHz with reflection coefficient of 23 dB and bandwidth of 0.3 GHz (0.7-1.0 GHz).
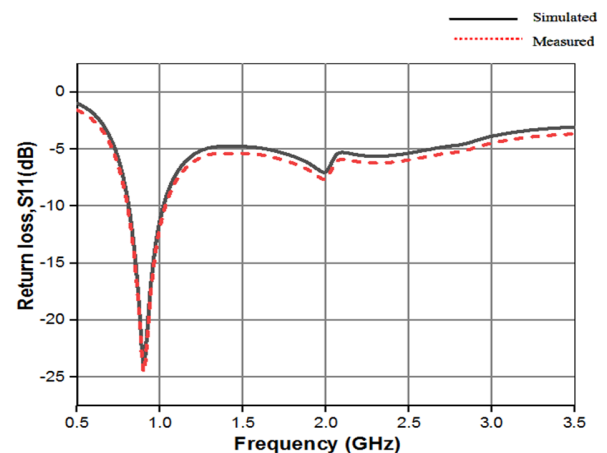

Fig. 5.   S11 of the simulated and fabricated serrated rectangular ESA.

The antenna was fabricated by utilizing chemical etching. For the measured antenna, a return loss of -22 dB at 0.92 GHz was observed. The source antenna is utilized as the standard for measurement, and is connected to the receiver end of the proposed antenna to obtain the measured S11. The radiation pattern of the serrated rectangular ESA was acquired in an anechoic chamber. In an anechoic chamber (Figure 3), the radiation pattern and peak gain of the serrated rectangular ESA were computed. Figure 7 illustrates the radiation pattern at the resonant frequency of 0.9 GHz of the simulated and the manufactured antennas. The serrated rectangular ESA is shown to have high radiation pattern performance and achieves a bidirectional pattern in both the H-plane and the E-plane.
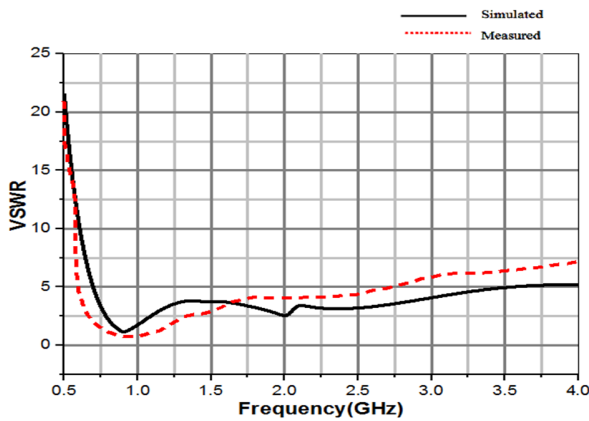
Figure 8 presents the observed peak gain at 0.9 GHz. In terms of peak gain and radiation efficiency, it is evident that the serrated rectangular ESA works well. Figure 6 depicts the antenna's VSWR, which is less than 2 at 0.9 GHz. Figure 10 displays the surface current distribution at the resonant frequency, where the coupling between the feed line and the patch results in the maximum current density of 170 A/m^2. We can observe that the current density increases after changing the structure by adding slots and utilizing defective ground because the maximum current density of the rounded rectangular patch without slots and DGS is 81 A/m^2. At 0.9 GHz, the serrated rectangular ESA achieves a gain of 1 dB, as shown in Figure 7.

Fig. 6.   VSWR of the simulated and fabricated serrated rectangular ESA.
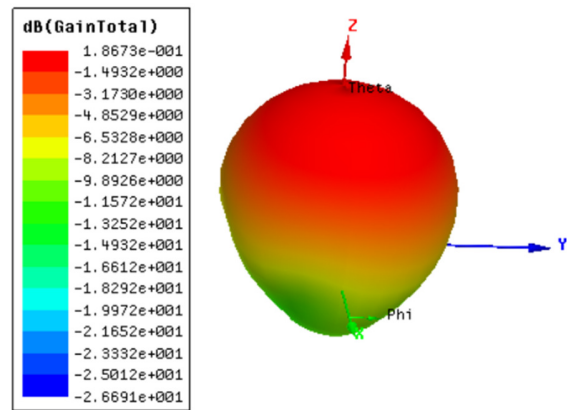

Fig. 8.   3D gain of the serrated rectangular ESA.

Fig. 7.   Serrated rectangular ESA's radiation pattern at 900MHz: (a) E-plane, (b) H-plane.
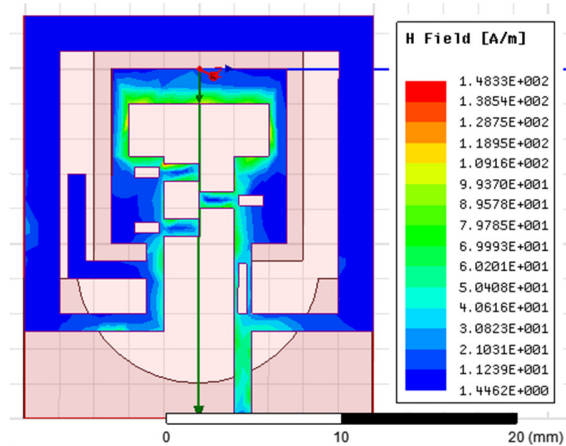

Fig. 9.   H field distribution of the serrated rectangular ESA.

Table II analyzes the proposed broadband antenna for RFID applications with a few antennas that have already been published in the literature. The antenna described in [4] has a relatively small return loss compared to the proposed antenna. The large antenna in [6] has a limited impedance bandwidth. The antenna in [8] is simpler to construct and has a lower return loss and VSWR. The antenna in [13] is larger and has a complex architecture printed in Taconic RF-35. The comparison demonstrates that, in terms of impedance bandwidth, antenna size, and gain, the proposed broadband antenna has a number of advantages over the previously reported antennas.
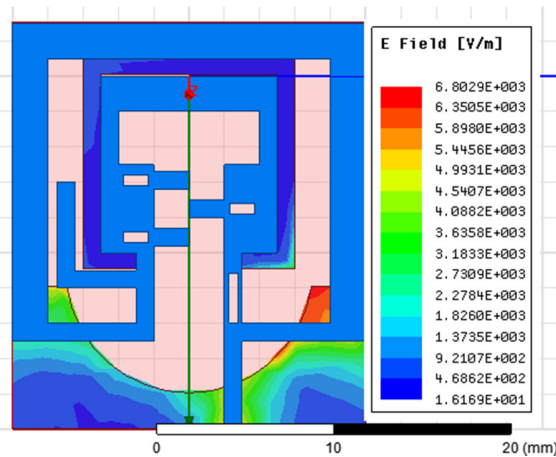
Fig. 10.   E field distribution of the serrated rectangular ESA.
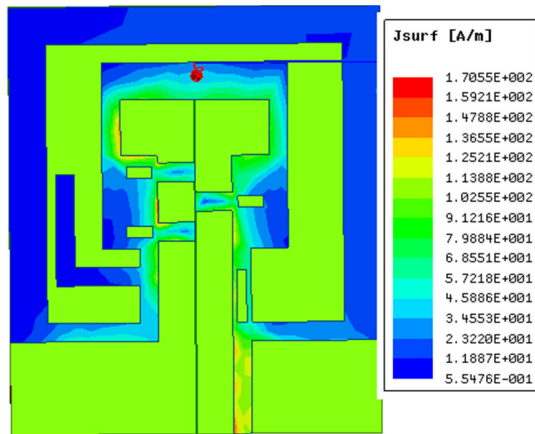

Fig. 11.   Surface current distribution of the serrated rectangular ESA.

TABLE II.   COMPARISON OF THE SERRATED RECTANGULAR ESA WITH ANTENNAS AVAILABLE IN THE LITERATURE

Ref	Antenna size (mm³)	Material used	Resonant frequency	Return loss	Gain	VSWR
[4]	60×60×1.6	FR4	870 MHz	-11.1 dB	0.4 dB	1.9
[6]	70×80×3.175	Rogers/RT Duroid 5880	890 MHz	-12 dB	0.8 dB	1.8
[8]	70×70×1.6	FR4	900 MHz	-17 dB	0.2 dB	1.5
[9]	60×60×1.5	Rogers/RT Duroid 5880	870 MHz	-14 dB	0 dB	1.8
[13]	70×20×0.5	Taconic RF-35	1.7 GHz	-18 dB	0.89 dB	1.7
Proposed	20×18×1.6	FR4	900 MHz	-23 dB	1.8 dB	1.25

IV.   CONCLUSION

Using the MS2037C Anritsu Combinational Analyzer, a compact, bidirectional ESA resonating at 900 MHz was designed, simulated, and tested. The serrated rectangular ESA has a simulated S11 of -23 dB at 900MHz. An ESA with a circular slot has a 300 MHz measured bandwidth for S11 <-10 dB. In terms of VSWR and S11, the simulated and measured results match each other well. Since the radiation pattern is bidirectional in both azimuthal and elevation angles, the recommended antenna is appropriate for RFID and mobile communication applications.

REFERENCES

[1] K. Finkenzeller, *RFID Handbook: Fundamentals and Applications in Contactless Smart Cards, Radio Frequency Identification and Near-Field Communication*, 1st ed. Chichester, West Sussex, UK ; Hoboken, NJ, USA: Wiley, 2010.

[2] K. V. S. Rao, P. V. Nikitin, and S. F. Lam, "Antenna design for UHF RFID tags: a review and a practical application," *IEEE Transactions on Antennas and Propagation*, vol. 53, no. 12, pp. 3870–3876, Sep. 2005, https://doi.org/10.1109/TAP.2005.859919.

[3] V. P. Plessky and L. M. Reindl, "Review on SAW RFID tags," *IEEE Transactions on Ultrasonics, Ferroelectrics, and Frequency Control*, vol. 57, no. 3, pp. 654–668, Mar. 2010, https://doi.org/10.1109/TUFFC.2010.1462.

[4] D. V. Kholodnyak, P. A. Turalchuk, A. B. Mikhailov, S. Yu. Dudnikov, and I. B. Vendik, "3D Antenna for UHF RFID Tags with Eliminated Read-Orientation Sensitivity," in *2006 European Microwave Conference*, Manchester, UK, Sep. 2006, pp. 583–586, https://doi.org/10.1109/EUMC.2006.281459.

[5] J. C. Lin, Ed., *Electromagnetic Fields in Biological Systems*, 1st ed. Boca Raton, FL, USA: CRC Press, 2016.

[6] S. Rao *et al.*, "Miniature implantable and wearable on-body antennas: towards the new era of wireless body-centric systems [antenna applications corner]," *IEEE Antennas and Propagation Magazine*, vol. 56, no. 1, pp. 271–291, Oct. 2014, https://doi.org/10.1109/MAP.2014.6821799.

[7] C. A. Balanis, *Antenna Theory: Analysis and Design*, 3rd ed. Hoboken, N.J, USA: Wiley, 2005.

[8] D. M. Dopkin, S. M. Weigand, and N. Iye, "Segmented Magnetic Antennas for Near-field UHF RFID," *Microwave Journal*, vol. 50, no. 6, Jun. 2007, Art. no. 96.

[9] A. L. Popov, O. G. Vendik, and N. A. Zubova, "Magnetic field intensity in near field zone of loop antenna for RFID systems," *Technical Physics Letters*, vol. 36, no. 10, pp. 882–884, Oct. 2010, https://doi.org/10.1134/S1063785010100032.

[10] O. G. Vendik and I. A. Pakhomov, "Electric-and magnetic-field strengths in the Fresnel zone of a microradiator formed by an electric and a magnetic dipole," *Technical Physics*, vol. 50, no. 11, pp. 1479–1484, Nov. 2005, https://doi.org/10.1134/1.2131958.

[11] A. Shvetsov *et al.*, "Choice of quartz cut for sensitive wireless SAW temperature sensor," in *2014 IEEE International Ultrasonics Symposium*, Chicago, IL, USA, Sep. 2014, pp. 1505–1508, https://doi.org/10.1109/ULTSYM.2014.0372.

[12] L. J. Chu, "Physical Limitations of Omni-Directional Antennas," *Journal of Applied Physics*, vol. 19, no. 12, pp. 1163–1175, Dec. 1948, https://doi.org/10.1063/1.1715038.

[13] P. A. Turalchuk, D. V. Kholodnyak, and O. G. Vendik, "A novel low-profile antenna with hemispherical coverage suitable for wireless and mobile communications applications," in *2008 Loughborough Antennas and Propagation Conference*, Loughborough, UK, Mar. 2008, pp. 337–340, https://doi.org/10.1109/LAPC.2008.4516935.

[14] I. Govardhani *et al.*, "Design of high directional crossed dipole antenna with metallic sheets for UHF and VHF applications," *International Journal of Engineering & Technology*, vol. 7, no. 1.5, pp. 42–50, 2018, https://doi.org/10.14419/ijet.v7i1.5.9120.

[15] G. Imamdi, M. Narayan, A. Navya, and A. Roja, "Reflector array antenna design at millimetric (mm) band for on the move applications," *ARPN Journal of Engineering and Applied Sciences*, vol. 13, no. 1, pp. 352–359, Jan. 2018.

[16] G. Immadi *et al.*, "Analysis of substrateintegrated frequency selective surface antenna for IoT applications," *Indonesian Journal of Electrical Engineering and Computer Science*, vol. 18, no. 2, pp. 875–881, May 2020, https://doi.org/10.11591/ijeecs.v18.i2.pp875-881.

[17] M. N. Kumar *et al.*, "Analysis of a low-profile, dual band patch antenna for wireless applications," *AIMS Electronics and Electrical Engineering*, vol. 7, no. 2, pp. 171–186, 2023, https://doi.org/10.3934/electreng.2023010.

[18] K. H. Reddy, M. V. Narayana, G. Immadi, P. Satyanarayana, K. Rajkamal, and A. Navya, "A Low-profile Electrically Small Antenna with a Circular Slot for Global Positioning System Applications," *Progress In Electromagnetics Research C*, vol. 133, pp. 27–38, 2023, https://doi.org/10.2528/PIERC23021601.

[19] H. R. Katireddy, M. V. Narayana, and G. Immadi, "Innovative Design and Analysis of an Electrically Small Reconfigurable Antenna for GPS and Blue Tooth Applications," *Engineering, Technology & Applied Science Research*, vol. 11, no. 5, pp. 7684–7688, Oct. 2021, https://doi.org/10.48084/etasr.4465.

[20] M. O. Dwairi, "Increasing Gain Evaluation of 2×1 and 2×2 MIMO Microstrip Antennas," *Engineering, Technology & Applied Science Research*, vol. 11, no. 5, pp. 7531–7535, Oct. 2021, https://doi.org/10.48084/etasr.4305.

[21] S. Sarade and S. D. Ruikar, "Development of a Wide Bandwidth Massive Eight Dissimilar Radiating Element Multiband MIMO Antenna for mm-Wave Application," *Engineering, Technology & Applied Science Research*, vol. 12, no. 5, pp. 9166–9171, Oct. 2022, https://doi.org/10.48084/etasr.5133.

[22] M. Venkateswara Rao, B. T. P. Madhav, J. Krishna, Y. Usha Devi, T. Anilkumar, and B. Prudhvi Nadh, "CSRR-loaded T-shaped MIMO antenna for 5G cellular networks and vehicular communications," *International Journal of RF and Microwave Computer-Aided Engineering*, vol. 29, no. 8, 2019, Art. no. e21799, https://doi.org/10.1002/mmce.21799.

[23] K. V. Vineetha, P. R. Kumar, A. N. Babu, J. B. Naik, B. T. P. Madhav, and S. Das, "Investigations on Complementary Split Ring Resonator (CSRR) array integrated printed conformal band pass filters for modern wireless communication applications," *Journal of Instrumentation*, vol. 17, no. 10, Jul. 2022, Art. no. P10043, https://doi.org/10.1088/1748-0221/17/10/P10043.

[24] M. Najumunnisa *et al.*, "A Metamaterial Inspired AMC Backed Dual Band Antenna for ISM and RFID Applications," *Sensors*, vol. 22, no. 20, Jan. 2022, Art. no. 8065, https://doi.org/10.3390/s22208065.

[25] S.-M. Chiang, E.-H. Lim, P.-S. Chee, Y.-H. Lee, and F.-L. Bong, "Dipolar Tag Antenna With a Top-Loading Inductive Channel With Broad Range Frequency Tuning Capability," *IEEE Transactions on Antennas and Propagation*, vol. 70, no. 3, pp. 1653–1662, Mar. 2022, https://doi.org/10.1109/TAP.2021.3111093.

[26] M. Murugesh, E.-H. Lim, P.-S. Chee, and F.-L. Bong, "Complementarily Coupled C-Shaped Microstrip Patches With Wide-Range Frequency Tuning Capability for Metal-Applicable UHF RFID Tag Design," *IEEE Transactions on Antennas and Propagation*, vol. 70, no. 12, pp. 11548–11558, Sep. 2022, https://doi.org/10.1109/TAP.2022.3209733.

[27] T. Althobaiti, A. Sharif, J. Ouyang, N. Ramzan, and Q. H. Abbasi, "Planar Pyramid Shaped UHF RFID Tag Antenna With Polarisation Diversity for IoT Applications Using Characteristics Mode Analysis," *IEEE Access*, vol. 8, pp. 103684–103696, 2020, https://doi.org/10.1109/ACCESS.2020.2999256.

[28] W.-H. Ng, E.-H. Lim, F.-L. Bong, and B.-K. Chung, "Compact Folded Crossed-Dipole for On-Metal Polarization Diversity UHF Tag," *IEEE Journal of Radio Frequency Identification*, vol. 4, no. 2, pp. 115–123, Jun. 2020, https://doi.org/10.1109/JRFID.2020.2965282.

[29] N. Ambati, G. Immadi, M. V. Narayana, K. R. Bareddy, M. S. Prapurna, and J. Yanapu, "Parametric Analysis of the Defected Ground Structure-Based Hairpin Band Pass Filter for VSAT System on Chip Applications," *Engineering, Technology & Applied Science Research*, vol. 11, no. 6, pp. 7892–7896, Dec. 2021, https://doi.org/10.48084/etasr.4495.